Comparison of Electrodeposited and Sputtered Tungsten Trioxide Films for Inorganic Electrochromic Nanostructures

Downloaded from: https://research.chalmers.se, 2025-12-04 19:58 UTC

Citation for the original published paper (version of record):
Gugole, M., Olsson, O., Gupta, V. et al (2023). Comparison of Electrodeposited and Sputtered Tungsten Trioxide Films for Inorganic
Electrochromic Nanostructures. ACS Applied Optical Materials, 1(2): 558-568.
http://dx.doi.org/10.1021/acsaom.2c00133

N.B. When citing this work, cite the original published paper.

research.chalmers.se offers the possibility of retrieving research publications produced at Chalmers University of Technology. It covers all kind of research output: articles, dissertations, conference papers, reports etc. since 2004. research.chalmers.se is administrated and maintained by Chalmers Library

(article starts on next page)

ACS APPLIED OPTICAL MATERIALS

pubs.acs.org/acsaom

Article

Comparison of Electrodeposited and Sputtered Tungsten Trioxide Films for Inorganic Electrochromic Nanostructures

Marika Gugole, Oliver Olsson, Vandna K. Gupta, Romain Bordes, Elisabet Ahlberg, Anna Martinelli, and Andreas Dahlin*

Cite This: *ACS Appl. Opt. Mater.* 2023, 1, 558−568

Read Online

ACCESS | Metrics & More | Article Recommendations | Supporting Information

ABSTRACT: Electrochromic materials and their implementation with structural colors are currently being intensely researched because of their promising applications as non-emissive display devices utilizing ambient light. In particular, several fully inorganic devices that rely on electrochromic tungsten trioxide (WO_3) have been presented. For preparing nanoscale films of this material, sputtering is the most established technique, but electrodeposition has recently been shown to be capable of achieving exceptionally high electro-optical modulation contrast without the need for expensive equipment. In this work, we investigate the possibilities of electrodeposited WO_3 and present a systematic comparison with sputtered WO_3 with respect to performance in electrochromic devices. Importantly, we show that "ultralarge" electro-optical modulation (~95% change in transmission) is possible for both types of films. However, it is only the sputtered films that enable such high contrast in a stable electrolyte such as $LiClO_4$ in propylene carbonate. The electrodeposited films are less uniform and difficult to make thicker than ~500 nm. We find no evidence that the electrochromic properties of the electrodeposited WO_3 are intrinsically better than those of sputtered WO_3. However, the electrodeposited films are much rougher and/or porous on the nanoscale, which increases the switching speed considerably. We conclude that electrodeposited WO_3 is mainly useful in applications in which high contrast is not essential while switching speed is. As an example, we present the first electrodeposited WO_3 integrated with structural colors by sandwiching the material between two metal films. By electrical control, the reflective colors can then be tuned at least one order of magnitude faster (a few seconds) than previously reported while having fair color quality and without any loss of brightness.

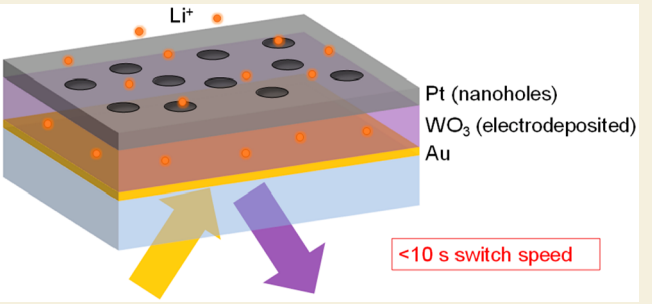

KEYWORDS: *tungsten trioxide, structural colors, electrochromism, nanostructures, Fabry-Pérot, thin films*

Downloaded via CHALMERS UNIV OF TECHNOLOGY on December 13, 2023 at 15:02:27 (UTC).
See https://pubs.acs.org/sharingguidelines for options on how to legitimately share published articles.

INTRODUCTION

The combination of solid electrochromic materials and structural colors has been the subject of intense research in recent years with many potential applications.[1−8] The main motivation is to develop energy-saving displays that reflect ambient light instead of relying on emissive pixels (as in ordinary liquid crystal displays or light-emitting diode displays). Although combinations of electrochromic materials can provide a full color range,[9] the integration with structural coloration in ultrathin layers is viewed as a possibility for more vibrant colors and higher contrast. Metallic nanostructures are particularly useful as they also readily act as electrodes for switching the electrochromic material. Broadly, one can define the range of electrochromic devices as based on either organic materials such as conjugated polymers or inorganic metal oxides.[7] Both types alter their colors in a similar manner in electrochemical cells, although the mechanisms of ion intercalation may differ. Inorganic materials normally switch slower but are expected to provide long device lifetimes by being robust toward chemical degradation.[4] Among the inorganic electrochromic materials, oxygen deficient tungsten trioxide (WO_3) is most commonly used due to its high-contrast broadband switching capability over the visible; i.e., the material is either highly transparent or black.

WO_3 films have been prepared by many quite different methods,[10−13] but today the most popular technique is arguably sputtering, which is also preferred in industry.[14] Sputtering means deposition by a reactive (oxygen-containing) plasma and a metallic tungsten source (Scheme 1A). Despite its obvious success and compatibility with large areas, sputtering and other vacuum deposition methods require expensive equipment that may not be available to all scientists or engineers working with electrochromic devices. An

Received: October 19, 2022
Accepted: January 5, 2023
Published: January 25, 2023

© 2023 The Authors. Published by American Chemical Society

Scheme 1. Main Methods of WO_3 Film Preparation Investigated Herein: (A) Reactive Sputtering[15] with a Metallic W Source and (B) Electrodeposition[16] Using a Conductive Surface Material

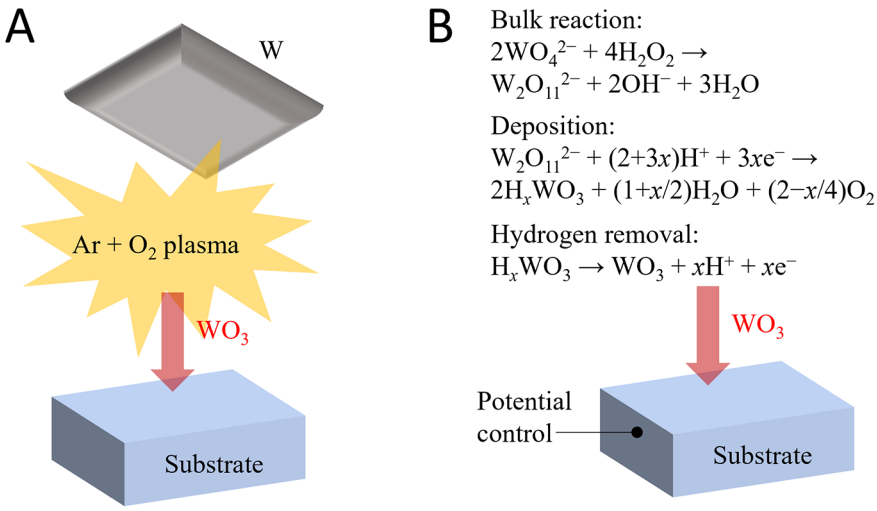

interesting alternative that does not require advanced equipment is electrochemical deposition methods, where reductive potentials are used to induce the formation of WO_3 films from tungsten salts in the solution phase. Such electrodeposition is conceptually similar to how conductive polymers can be conveniently prepared by electropolymerization directly on fabricated nanostructures or electrodes.[15] Importantly, electrodeposition (Scheme 1B) was recently shown to provide WO_3 films with exceptionally high optical switching contrast by Cai et al.[16] This shows that the preparation of WO_3 films for various electro-optical applications, while having been investigated for many years,[11] remains a contemporary topic. In fact, it may be even more important than ever due to the recent interest in using WO_3 for active tuning of optically resonant nanostructures.[17−23] In comparison with the widely used sputtered films, few studies have investigated the electrochromic performance of electrodeposited WO_3. Specifically, the conditions under which electrodeposition of WO_3 can be superior to the established method of sputtering need to be clarified, in addition to how differences can be utilized for optimal tuning of structural colors.[4]

In this work, we investigate in detail the usefulness of electrodeposited WO_3 and show in which cases it may be beneficial over sputtered films for electrochromic devices. We consider several aspects such as contrast, switching speed, and lifetime in different electrolytes. The thickness of both types of films is varied, and the influence on switching performance analyzed. The role of film morphology is shown to be particularly important. Overall, the electrodeposited WO_3 is not superior to sputtered films but may become useful in specific cases. To illustrate this, we prepare electrochromic Fabry-Pérot cavities using WO_3 as a sandwiched layer, showing the first implementation of electrodeposited WO_3 for tuning of structural colors. Remarkably, this gives an improvement in switching speed of over one order of magnitude. Our study serves as a guideline for preparing devices based on inorganic electrochromism with optimal performance depending on context.

EXPERIMENTAL SECTION

Preparation of WO_3 Films

Indium tin oxide (ITO)-coated glass (Naranjo) was used as the substrate. Reactive RF sputtering of WO_3 was performed using a Nordiko 2000 system as previously reported.[15] Electrodeposition of WO_3 was performed using a three-electrode setup with a Ag/AgCl reference electrode (immersed in 3 M KCl), a Pt counter electrode, and a Gamry Interface 1010E potentiostat in an open beaker. The deposition was carried out in a solution containing 250 mL of Milli-Q water and 1.0995 g (13 mM) of $Na_2WO_4{\cdot}2H_2O$, acidified using 0.5 M sulfuric acid to pH 1.3, and finally, 0.647 mL of 30% (w/v) H_2O_2 was added. The solution was left at room temperature for several days before use.[13] The deposition sequence was comprised of 0.1 s at −0.7 V, 0.1 s at 0 V, and a 0.1 s pause at the open circuit to create WO_3. The pause was necessary to create films with good performance (high contrast). During deposition, the solution was stirred at 600 rpm. Sol−gel deposition was performed as described by Inamdar et al.[24] In brief, 1 g of WCl_6 was dissolved in 10 g of absolute EtOH and stirred for 4 h. The blue solution was pushed through a 0.2 μm polypropylene filter and spin-coated on the ITO slides after which they were cured on a hot plate (70 °C) for 30 min. Chemicals were from Sigma-Aldrich.

Thickness Measurements

The thicknesses of the WO_3 films were measured using a KLA Tencor Alpha-Step D-100 profilometer with a tip having a 2.5 μm radius of curvature. A reference region for enabling the step in the profilometer measurement was obtained by masking part of the sample during deposition with tape.

Electrochemical Measurements

The samples were mounted in a custom-made spectro-electrochemical cell (RedoxMe AB) connected to the potentiostat. The electrochemical switching was carried out between −0.7 and 0.7 V for the electrodeposited films and between −0.7 and 1 V for the sputtered films. (Increasing the anodic voltage to 1.0 V for the electrodeposited films did not improve the contrast.) The reference electrode was Ag/AgCl in contact with LiCl in ethanol except when using an aqueous electrolyte, in which case it was in contact with KCl (separated from the bulk electrolyte). Impedance spectra were recorded with an amplitude of 25 mV and a DC offset of −1.0 V using a Gamry Reference 600+. The experimental data were fitted against an equivalent circuit using the ZView software from Scribner Associates.

https://doi.org/10.1021/acsaom.2c00133
ACS Appl. Opt. Mater. 2023, 1, 558−568

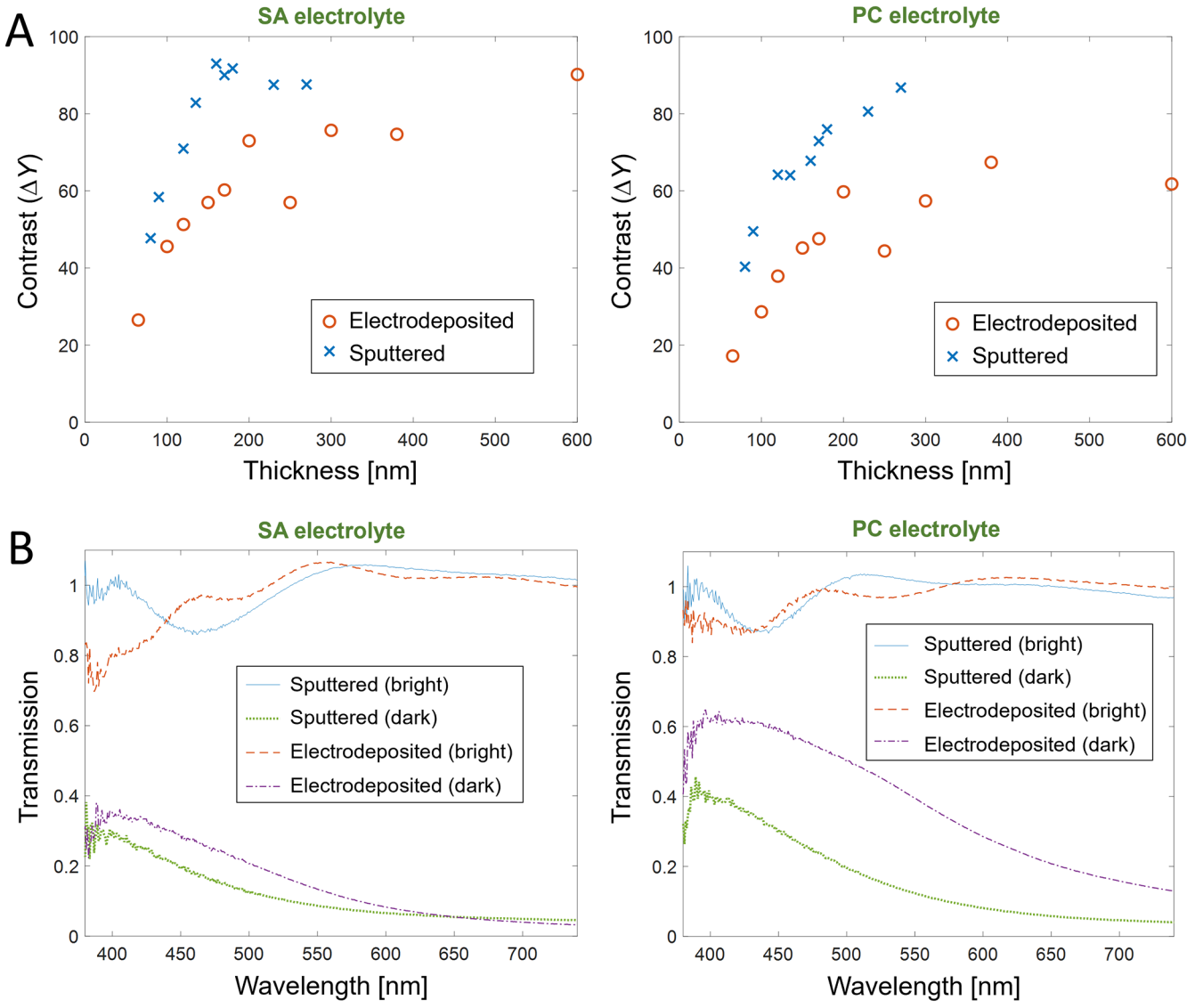

Figure 1. Optical contrast for different film thicknesses. (A) Contrast calculated as the difference in transmittivity weighted with the luminosity function for different film thicknesses. Electrodeposited and sputtered WO_3 films on ITO are compared in two different electrolytes (SA, 0.5 M H_2SO_4; PC, 1 M $LiClO_4$ in propylene carbonate). Each data point represents one sample. The measurement error (at least in the initial cycles) is smaller than the symbols. (B) Transmission spectra of bright and dark states of sputtered and electrodeposited WO_3 films in either electrolyte. The thicknesses of the films were those that gave the highest contrast: 160 and 270 nm for sputtered films in SA and PC, respectively, and 600 nm for the electrodeposited film, for both electrolytes. Note that the transmission slightly exceeds 100% for some wavelengths in the bright state. This is due to thin film interference and the fact that the reference intensity was measured through exactly the same materials except the WO_3, i.e., glass, ITO, and the electrolyte. The measurement variation when switching a sample is <1% in *T*.

Optical Measurements

A home-built microscopy/reflection setup was used[15] with a 4× air objective (NA 0.1, angular range of ≤4°) for illumination and collection of reflected light. A tungsten lamp (Azpect Photonics) was used, and the spectrometer was a fiber-coupled photodiode array (B&WTek). For reflection measurements, a broadband dielectric mirror (BB05-E02, Thorlabs) was used as a reference. For transmission measurements, the reference was the same type of ITO substrate placed in the electrochemical cell and immersed in the electrolyte.

Fabrication of Nanostructures

Au−WO_3−Pt nanocavities were fabricated in a manner similar to that described previously.[17] WO_3 was deposited on the semitransparent 20 nm Au layer. Ti and Pt were evaporated after colloidal lithography with 140 nm polystyrene sulfate particles (Microparticles Gmbh). The particles were stripped using tape. For the case of electrodeposited WO_3, the thickness of the Pt mirror was slightly reduced (65 nm instead of 70 nm) and a 5 nm Ti adhesion layer was used between WO_3 and Pt to ensure that the mirror did not peel off. (Most likely, the higher roughness of the electrodeposited WO_3 is the reason why these minor changes were necessary.) The transmission through the colored nanostructures was still only ∼1% when using a 65 nm Pt mirror. Note that the structural colors were observed through the glass support; i.e., a reversed design was used.[17]

Atomic Force Microscopy (AFM)

AFM imaging was performed in air on an NTEGRA Prima instrument (NT-MDT) working in tapping mode using a NSG01 probe (NT-MDT), and the pictures were processed using Gwyddion.

https://doi.org/10.1021/acsaom.2c00133
ACS Appl. Opt. Mater. 2023, 1, 558−568

Infrared (IR) and Raman Spectroscopy

FTIR spectra of the WO_3 films were recorded in the attenuated total reflectance mode using a PerkinElmer Frontier spectrometer, at room temperature. The step length was 0.1 cm^{-1}, and the spectral resolution was 4 cm^{-1}. Raman spectra of the WO_3 films were recorded at room temperature using a WITec alpha300 R spectrometer equipped with an air-cooled CCD detector and using a 532 nm laser. The spatial and spectral resolutions achieved with this experimental setup were 0.9 μm and 3 cm^{-1}, respectively. The spectra were recorded at several spots (20−25 spots) within a sample area of 80 μm × 80 μm. For each spectrum, the acquisition time was ∼3 s using five accumulations. The laser power was 1 mW unless otherwise stated. The objective used was a Zeiss EC EPIPLAN 50× lens with a numerical aperture of 0.75.

X-ray Diffraction

The spectra were acquired between 2θ values of 15° and 70° on a Bruker D8 Discover diffractometer in a θ−2θ configuration, equipped with a Cu tube X-ray source and an Eiger2 R 500K two-dimensional detector set to one-dimensional mode. Samples were mounted on standard holders. Data were acquired in 0.02° increments with a 7 s exposure per step. The motorized divergence slit on the incoming beam side was set to fixed sample illumination mode with a 5 mm sample length, and an air scattering shield was placed 3 mm above the sample. Samples were rotated at 10 rpm.

RESULTS AND DISCUSSION

We prepared sputtered WO_3 films as described previously,[15] while electrodeposited WO_3 was prepared using similar voltage pulses and reagents as described by Cai et al.[16] An important parameter that always influences the electrochromic performance of the film (regardless of how it is prepared) is the thickness.[15] In this work, all film thicknesses were measured with a profilometer. Electrochemical switching was performed in a three-electrode setup (Ag/AgCl reference and Pt counter) using electrolytes consisting of either sulfuric acid (SA, 0.5 M H_2SO_4) or 1 M $LiClO_4$ in propylene carbonate (PC). These are the electrolytes that are normally used for WO_3 switching, providing either H^+ or Li^+ intercalation at reductive potentials, which makes the material turn from transparent to absorbing over the visible range.

We first consider the highest contrast that could be achieved with the different types of WO_3 films. For a simple absorbing film in which interference effects can be ignored, there is an optimal thickness that gives the highest contrast when it is defined as the difference in transmission.[15] (In reflection mode, this thickness is simply reduced by a factor of 2 because light passes through twice.) Note that because WO_3 has a high real part of its refractive index[25] (RI), interference effects may be noticeable and the "absorption only" (Lambert−Beer) model is not expected to fully fit the data.[15] Furthermore, to obtain a contrast that takes into account the full spectrum and the sensitivity of the eye, one can use a normalized transmission change:

$$\Delta Y = \frac{\int_{380\ \mathrm{nm}}^{780\ \mathrm{nm}} L(\lambda)\Delta T(\lambda)\ \mathrm{d}\lambda}{\int_{380\ \mathrm{nm}}^{780\ \mathrm{nm}} L(\lambda)\ \mathrm{d}\lambda} \times 100$$

where L is the luminosity function as obtained from Commission Internationale de l'Éclairage (CIE). Clearly, ΔY is important for electrochromic applications, but the ΔT value at a selected wavelength may still be the most important benchmark parameter in other active devices.

Figure 1 shows plots of contrast versus film thickness for electrodeposited and sputtered WO_3 films in the different electrolytes. A clear trend of increased contrast with thickness can be identified in all cases, which eventually reaches an optimum or at least stops to increase significantly. This occurs for smaller thicknesses in the SA electrolyte compared to PC, which can be attributed to differences in intercalation behavior for H^+ versus Li^+. Although the change in optical properties should be the same regardless of the intercalating cation,[26,27] the protons are smaller and there should be more intercalation sites available for them inside the WO_3. Thus, it is expected that a smaller film thickness is sufficient to reach the highest contrast for the case of proton intercalation. However, this does not strongly influence the ΔY values that can be reached, which are similar for both electrolytes (Figure 1A). Still, it is noteworthy that the electrodeposited films generally exhibited lower contrast. Figure 1B shows the full spectra at the thicknesses that correspond to the highest ΔY. The spectral shapes are clearly very similar regardless of electrolyte and film preparation method. The major difference is the relatively high transmission of the dark state for electrodeposited WO_3 in the PC electrolyte, confirming a relatively small amount of Li^+ intercalation. Also, for the electrodeposited film, which is 600 nm thick, several maxima and minima can be seen in the spectra due to thin film interference. However, they are less pronounced than what is predicted for a smooth homogeneous film (Figure S1), suggesting a more heterogeneous morphology.

We also investigated a sol−gel method for producing WO_3,[24] which is similar to electrodeposition in the sense that ionic W species in solution are reduced. Although this is an easy method to perform (only a spin coater is needed), sol−gel films cannot be prepared selectively on electrodes by potential control. Furthermore, we did not find that these WO_3 films exhibited better performance (Figure S2).

Importantly, we can now compare our WO_3 films to those with "ultralarge" contrast in the work by Cai et al.,[16] which exhibited a transmission change of almost 98% at 633 nm. Our spectra confirm that the contrast is highest in the red region and our maximum (single wavelength) ΔT value is identical for the SA electrolyte (Figure 1B), which was also used by them. However, obtaining this contrast requires the thickest electrodeposited film we could prepare. Above a thickness of ∼400 nm, it was increasingly difficult to prepare electrodeposited films in a reproducible manner while maintaining good adhesion to the surface. Consequently, an equally large change in transmission could not be reached in the PC electrolyte (ΔT of 70−80% in the red region). Even for the thickest film that we managed to prepare, the dark state was still relatively transmissive due to the lower degree of ion intercalation (Figure 1B). We also noted poorer uniformity for the electrodeposited films (Figure S3), which complicates their use for large-area electrochromic devices. In comparison, for the sputtered films, the maximum contrast is at least as high in SA and an almost equally high ΔT (93% at 638 nm) can be obtained in PC, which was not possible for any of the electrodeposited films. The PC is a redox-stable nonvolatile liquid more suitable for most applications than aqueous electrolytes.[28]

The fact that the electrodeposited and sputtered WO_3 films differ with respect to the thickness at which the highest contrasts were obtained (Figure 1A) may be due to differences in the film morphology. If the electrodeposited films are porous, as expected,[16] they effectively contain less WO_3 and therefore a thicker film will be needed to reach the optimal

https://doi.org/10.1021/acsaom.2c00133
ACS Appl. Opt. Mater. 2023, 1, 558−568

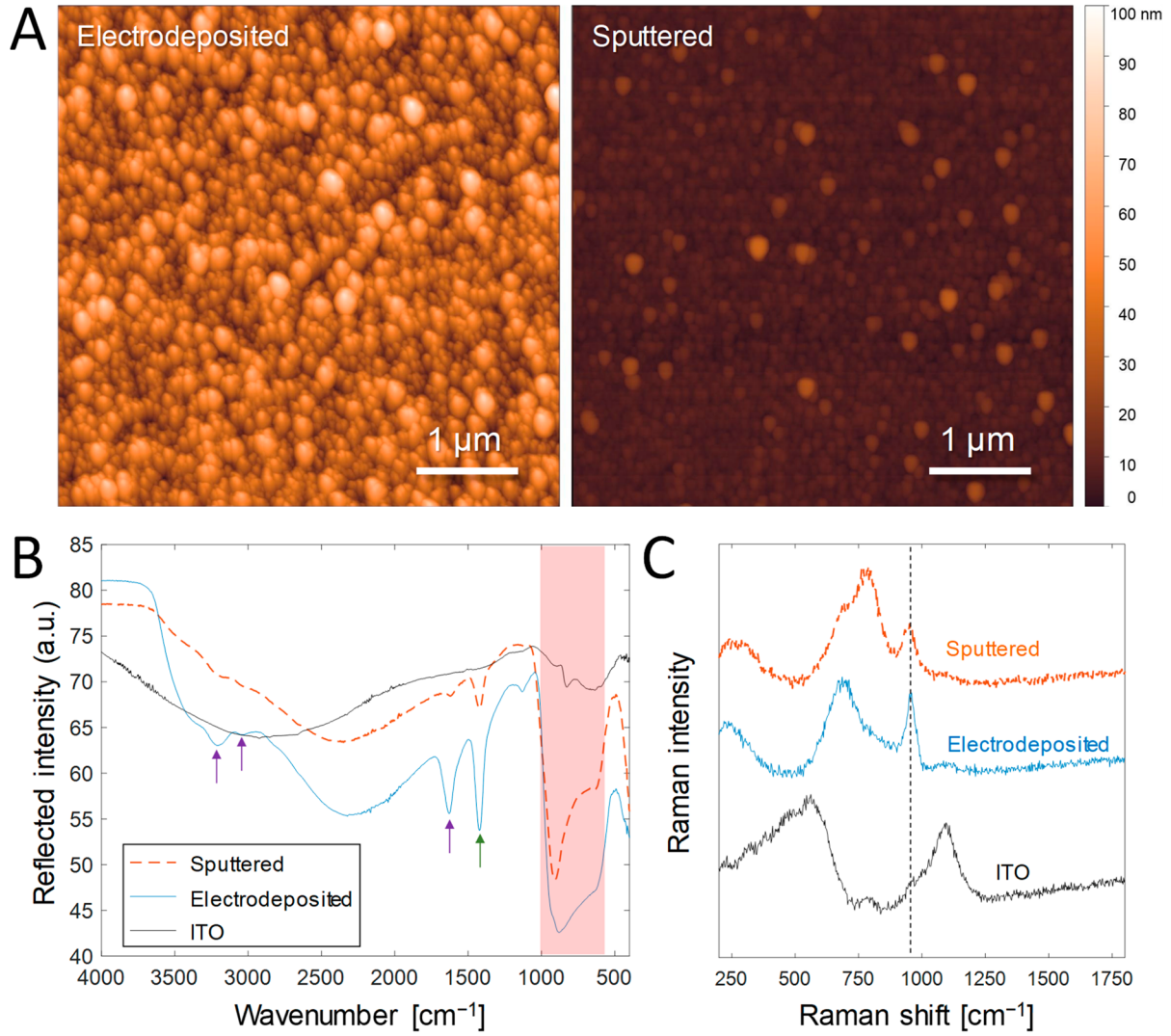

Figure 2. Film characterization. (A) Atomic force microscopy images of electrodeposited and sputtered WO_3 films. Note that the color scale is the same. Both films had the same thickness (as measured by the profilometer) of 160 nm. (B) FTIR spectra measured in the attenuated total reflection configuration. WO_3 absorption is expected in the marked interval. Purple arrows show water bands. The green arrow indicates a peak observed previously for aged WO_3 films.[32] The film thickness was 270 nm for sputtered and 600 nm for electrodeposited WO_3. (C) Raman spectra of the same samples as for FTIR. The W═O stretching mode at 955 cm^{-1} is indicated. The reproducibility of the determined peak positions was ±0.8 nm.

contrast. To investigate this, we recorded AFM images of the two types of WO_3 (Figure 2A). Indeed, the electrodeposited films were much rougher, 9.48 ± 1.18 nm versus 1.80 nm ± 0.67 nm for the sputtered films. Furthermore, the small protrusions on the surface occur quite frequently; i.e., they are separated by short distances (~100 nm). This means that the profilometer tip, which is much blunter (radius of curvature of 2.5 μm) than the AFM tip, will most likely sense the top of the protrusions. This, in turn, explains why the thicknesses that give the best contrast are different compared to those of the sputtered films. The amount of WO_3 on the surface is simply smaller for the electrodeposited films, even if the profilometer measures the same thickness. We note that for sputtered films, the surface roughness may increase when the film thickness approaches ~1 μm.[29] However, all of our films are considerably thinner than this, and Figure 2 compares two films with the same thickness.

Complementary to the AFM data, we also analyzed the films by other methods. FTIR spectra showed the characteristic WO_3 absorption bands in the region of 600−1000 cm^{-1}, which looked very similar for electrodeposited and sputtered films (Figure 2B). The broad spectral features indicate that both films were to a large extent amorphous.[30] Vibrational modes related to water[31] appear at 3200, 3040, and 1620 cm^{-1} and are slightly more intense for the electrodeposited films, suggesting the presence of bound water. This can be explained by the fact that an aqueous electrolyte is used for the electrodeposition. The vibrational mode at 1420 cm^{-1}, visible for both films, has previously been observed for aged WO_3 samples.[32] Additional characterization performed by Raman spectroscopy confirmed these results, revealing vibrational modes in the same spectral region (Figure 2C) albeit with a higher spectral resolution. For instance, the W═O stretching mode at 955 cm^{-1} is more clearly resolved. The sputtered and electrodeposited films both show spectra that indicate a hydrated amorphous phase, as

https://doi.org/10.1021/acsaom.2c00133
ACS Appl. Opt. Mater. 2023, 1, 558−568

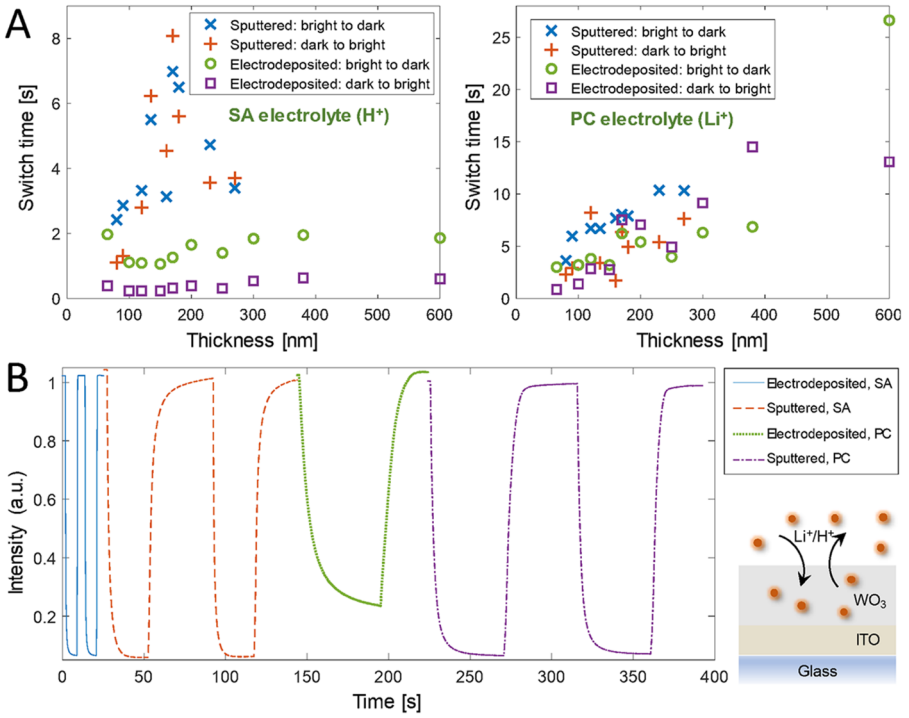

Figure 3. Switching speed analysis. (A) Time required to reach 90% of the total intensity change vs film thickness for the two different electrolytes. The switch times are separated with respect to WO_3 type and direction (bright to dark for ion intercalation and dark to bright for removing ions). Each point represents one sample. The measurement error was approximately ±1 s. (B) Switching dynamics for the film thicknesses that gave the optimal contrast (same as in Figure 1B). Note that the intensity units are arbitrary, but the curves can still be compared with each other.

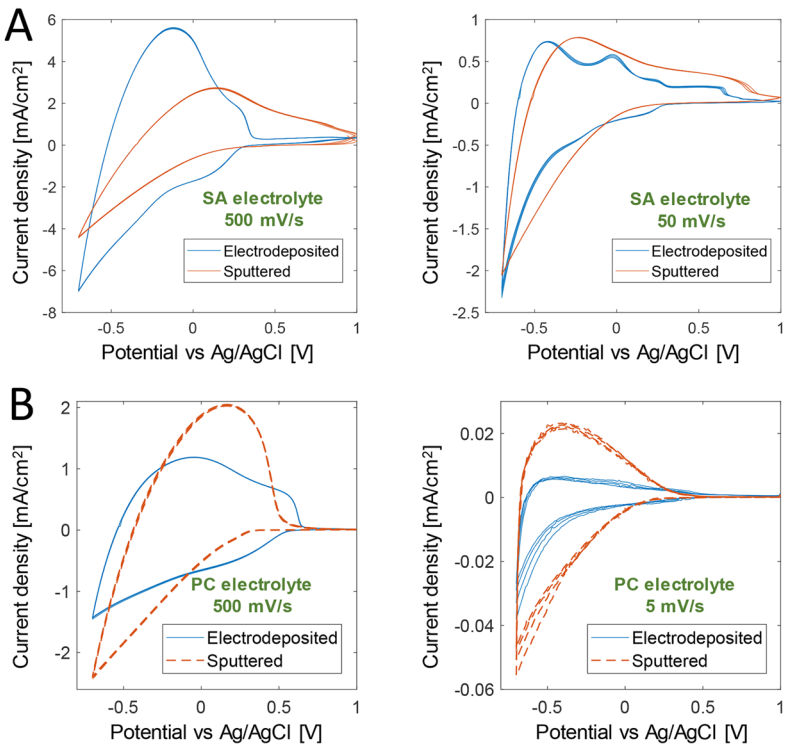

Figure 4. Cyclic voltammograms. (A) Sweeps in the SA electrolyte at 500 or 50 mV/s. (B) Sweeps in the PC electrolyte at 500 or 5 mV/s. In each case, four cycles are included. (Sweeping at 5 mV/s was not possible in the SA electrolyte due to extensive bubble formation.) The WO_3 thickness was 100 nm for the electrodeposited and 84 nm for the sputtered sample.

described by Santato et al.,[33] who studied mesoporous WO_3 films prepared by sol−gel deposition. The profile of the Raman spectra suggests that the electrodeposited films are more hydrated than the sputtered ones, in agreement with the results

https://doi.org/10.1021/acsaom.2c00133
ACS Appl. Opt. Mater. 2023, 1, 558−568

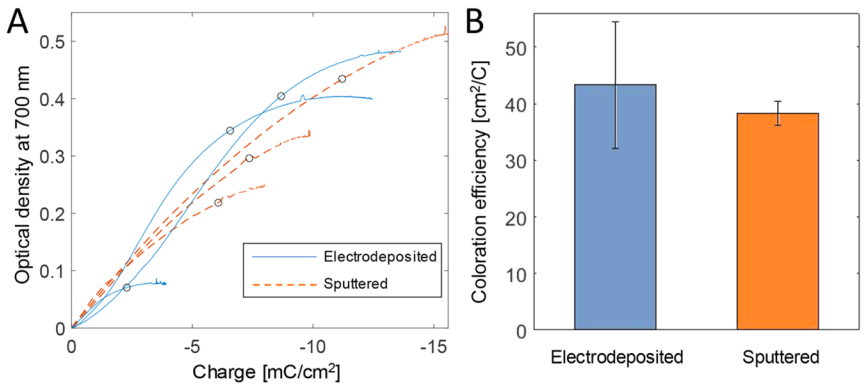

Figure 5. Coloration efficiency in the PC electrolyte. (A) Change in optical density (absorbance) at 700 nm plotted vs the integrated current during switching from bright to dark for electrodeposited and sputtered films of various thicknesses in the range 50−200 nm. The circles indicate when 90% of the total intensity change has been reached. (B) Mean coloration efficiency values from multiple samples based on the accumulated charge after reaching 90% of the total intensity change. The error bars represent two standard deviations.

from FTIR. We also noted that increasing the laser power led to annealing effects (due to local heating) for the electrodeposited WO_3 only, creating locally a monoclinic phase that exhibited a different Raman spectrum (Figure S4). This is again in agreement with the results presented by Santato et al.[33] Tentatively, the higher thermal stability of the sputtered films is also due to differences in film morphology. In any case, no samples were exposed to high temperatures during any of the other experiments.

It should be kept in mind that differences in exact W:O stoichiometry (oxygen deficiency) and crystalline orientation, none of which can be resolved well by FTIR or Raman, may also affect cation intercalation behavior.[24,25,34,35] Although we cannot exclude that there are some differences between sputtered and electrodeposited WO_3 with respect to these factors, X-ray diffraction data did not suggest large variation (Figure S5). Hence, we conclude that the most notable difference between sputtered and electrodeposited WO_3 is the film morphology. This conclusion was further supported by electrochemical impedance spectroscopy (EIS), which estimated the diffusivity of Li^+ ions in the films[36] (Figure S6).

Another important parameter for electrochromism is the switching speed. Figure 3 shows a summary of the switch time of sputtered and electrodeposited WO_3, defined as the time required to reach 90% of the total intensity change. The switch time generally increases with film thickness, as expected when the ions must be transported deeper into the material to reach intercalation sites. However, here our focus lies on differences that are due to the film preparation method. While inorganic electrochromic materials generally switch slower than conductive polymers, some reports have shown that increasing the porosity of WO_3 improves speed.[19] Thus, the larger surface area seen by AFM on the electrodeposited films is expected to contribute to an increased switching speed. Indeed, the electrodeposited films clearly switched faster than the sputtered WO_3 (Figure 3A), especially in the SA electrolyte. In PC, the switch time is generally longer and the electrodeposited films are not so much faster than the sputtered ones, especially when looking at the dark to bright switch (removal of intercalated Li^+). However, this is because a lower voltage was used for the electrodeposited films (0.7 V) when switching from dark to bright. We verified that increasing the voltage to the same value as for the sputtered films (1.0 V) led to faster switching, but not higher contrast (Figure S7). Thus, the electrodeposited films do switch faster in all cases, as expected from the larger effective surface area of the rough film, which simplifies access and movement for the ions. Notably, having a switching speed comparable to that of conductive polymers (~1 s) in both directions is only possible for electrodeposited WO_3 in the SA electrolyte. However, we again point out that the PC electrolyte is essential for applications in which the device needs a reasonably long lifetime (see below). Figure 3B shows examples of switching dynamics with the film thicknesses that provided the highest contrast. As explained above, the electrodeposited WO_3 in PC does not result in the same intensity change as the other three cases.

Cyclic voltammetry curves gave further insight into the differences between the WO_3 films (Figure 4). Approximately the same film thickness (~100 nm) was used for both sputtered and electrodeposited WO_3. First, we observed high currents at reductive potentials in the SA electrolyte (Figure 4A) due to hydrogen formation by reduction of protons (visible bubbles were quickly formed). This shows the complications of using this electrolyte for multiple switch cycles. Second, the redox activity is similar to or higher than that for the electrodeposited film at high sweep rates, but not when the sweep rate is decreased. In the PC electrolyte at 5 mV/s, it is instead the sputtered films that have more charge transfer per cycle (Figure 4B). This is in perfect agreement with the data on film morphology (Figure 2) and switching speed (Figure 3). The sputtered films are denser; i.e., there is more WO_3 available on the surface, which means that the number of intercalation sites is higher. This leads to a higher capacity for electron transfer, but only when the ion intercalation has sufficient time to reach saturation. Because the electrodeposited films switch faster, their redox activity can be higher for sufficiently fast scan rates. In other words, the CV results confirm that porosity is beneficial for fast ion transport through the film, but the switching capacity is reduced simply because there is less electrochromic material. We note that Cai et al.[16] found higher redox activity on more porous WO_3 films, but the influence of the scan rate was not reported. Additional oxidation and reduction peaks are visible for the electrodeposited WO_3, especially in the SA electrolyte. This was also observed by Cai et al.[16] and in earlier work, as well,[12] where it was attributed to different H^+ intercalation mechanisms.

https://doi.org/10.1021/acsaom.2c00133
ACS Appl. Opt. Mater. 2023, 1, 558−568

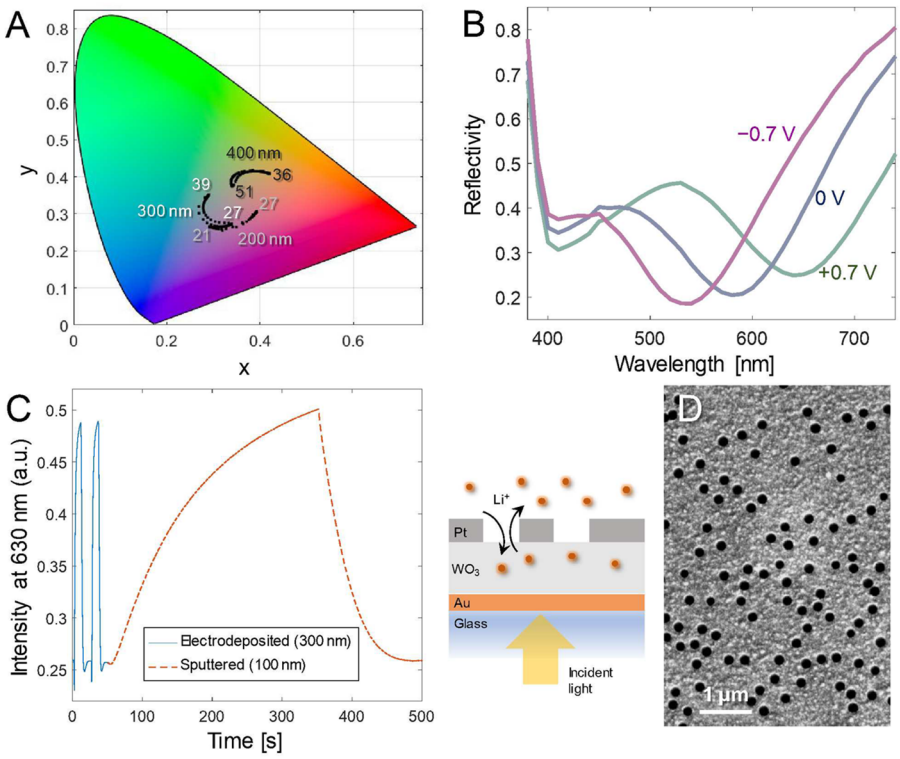

Figure 6. Electrochromic nanostructures with electrodeposited WO_3 between 20 nm Au and a Pt mirror. (A) Switching of samples visualized by the CIE diagram. Color changes for three different thicknesses are shown. The numbers are the brightness values (Y) measured at each end voltage. (B) Examples of spectra while switching a cavity with electrodeposited WO_3 (300 nm nominal thickness). Each line is pseudocolored on the basis of the measured spectrum. (C) Example of switching dynamics (intensity at 630 nm) in the PC electrolyte. The slower switch with sputtered WO_3 is included for comparison. Note that the electrodeposited film is thicker (but the nanostructures have a similar color). (D) Electron microscopy image of the Pt mirror with nanoholes (the backside of the structure) on top of electrodeposited WO_3.

Notably, the same effect is not observed for the sputtered films, which provide smoother curves in all cases.

The coloration efficiency (CE), i.e., the change in optical absorption per charge during switching, is another important parameter in electrochromism.[24] We did not observe any significant difference between electrodeposited and sputtered WO_3 films with respect to this parameter (Figure 5). This further suggests that the ion intercalation mechanisms are the same in both types of WO_3 and differences arise due to the film morphologies (Figure 2). However, the sample variation was larger for the electrodeposited samples, which could be related to the small additional redox activity observed in the CV curves for the electrodeposited films (Figure 4). As expected, the CE was not dependent on film thickness and the values are similar to what has been reported previously.[24]

We also investigated the lifetime of the devices, i.e., the preservation of contrast over multiple switching cycles.[37] In the SA electrolyte, lifetime measurements were not meaningful because the surface quickly became covered with bubbles (~10 cycles) that interfered with the optical readout. In the PC electrolyte, the switching was highly stable with small contrast loss even after ~1000 cycles for the voltage used for Li^+ intercalation (−0.7 V vs Ag/AgCl). No major differences in lifetime were observed for electrodeposited versus sputtered films (Figure S8). Both exhibited a loss of transparency for the bright state, as expected from trapped Li^+ ions.[37] Also, for both types of WO_3, it was possible to use a more negative voltage to enhance contrast and speed, but this led to more ion trapping and a poor lifetime, as expected.[38] (We found −0.7 V to be a good compromise.)

On the basis of the results described above, one can identify in which applications the electrodeposited WO_3 can be potentially more useful than sputtered films. We first note the (slightly banal) case in which one does not have access to a tool for reactive sputtering deposition. Other than that, we argue that the electrodeposited WO_3 is generally not suitable for ordinary intensity modulation unless switching speed is paramount. This is because sputtered films reach essentially the same high contrast (Figure 1), and it can be achieved using a much more stable electrolyte (PC instead of SA). However, the electrodeposited WO_3 can still be useful as the electrochromic material inside various types of resonant nanocavities, for instance, those providing resonant reflection in metal−insulator−metal geometries.[17,20,21,23] For these structures, the color is changing instead of being switched on or off, as when a WO_3 film is stacked on top of a colored nanostructure.[15] Thus, the electrochromic performance is mainly evaluated with respect to chromaticity and brightness (not contrast). In such cavities, the WO_3 film thickness will determine the color range that can be achieved with different degrees of ion intercalation. We hypothesized that the electrodeposited films could improve the performance of these structures, at least with respect to switching speed. Hence, we prepared nanostructures with electrodeposited WO_3 sandwiched between a semitransparent 20 nm gold film and a reflective Pt mirror with nanoholes that allow ions to pass. As we previously showed,[17] this design is advantageous because the counter electrode can be placed

https://doi.org/10.1021/acsaom.2c00133
ACS Appl. Opt. Mater. 2023, 1, 558−568

behind the reflective nanostructure, thereby increasing the brightness for the viewer.

Figure 6 shows examples of our electrochromic nanostructures with different thicknesses of electrodeposited WO_3. Here the PC electrolyte was used for long-term stability in the switching. (In fact, the nanostructures were even destroyed in SA, showing again the importance of not relying on this electrolyte.) Overall, compared with our previous work,[17] the brightness values in the different coloration states as represented by the Y parameter (white numbers in Figure 6A) are slightly higher (at least 10%). Although this is strongly dependent on which specific colors the cavities exhibit, the brightness seems not to be reduced when using electrodeposited WO_3. However, the chromaticity is slightly decreased; i.e., the curves do not reach quite as far across the CIE diagram as for sputtered WO_3 (see an example in Figure S9). This can be attributed to the increased film roughness, which will broaden the cavity resonance (as it depends strongly on thickness) in comparison with that of a smooth film, yet the color quality is still good in comparison with, for instance, commercial electronic paper in color.[17] Figure 6B shows reflectivity spectra obtained at different voltages for a 300 nm electrodeposited cavity, corresponding to green, blue, and purple colors.

Looking at the switching speed, we found that the nanostructures with electrodeposited WO_3 could switch at least one order of magnitude faster. The longest color switch, i.e., going from one end voltage state to the other, required <10 s. This is to be compared with switching times of several minutes for the sputtered films (Figure 6C), even though the cavity consisting of sputtered WO_3 is thinner. A video showing the fast switching is included in the Supporting Information. Note that the transport of ions through the nanoholes in Pt also affects the switching speed, but here we focus specifically on comparing the two types of WO_3 films. In agreement with the results described above (Figure 3), the large switching speed enhancement can to a high extent be explained by the more porous structure of the electrodeposited WO_3. Indeed, to generate the same structural color (reflectivity maximum at the same wavelength), the film thickness (300 nm) needed to be around 3 times higher compared to that of sputtered WO_3 (100 nm). Because it is not compact, the electrodeposited film needs to be thicker to create the same optical path length, i.e., the product of the RI and the distance between the metals, which must be similar when the colors are similar. However, when the effective RI of the cavity is being approximated on the basis of the values for WO_3[25] and PC,[15] it is not reasonable that the electrodeposited cavity is 3 times thicker. Thus, the deposited Pt is not forming a planar film "balancing" on top of the protrusions (Figure 2). Rather, it is at least to a large extent conformal to the underlying WO_3 film; i.e., the average cavity thickness must be <300 nm in reality.

CONCLUSION

We have evaluated the use of electrodeposited WO_3 films for electrochromic applications and for the first time implemented them for tuning of structural colors, with particular focus on comparing them with sputtered films. One of our most important findings is that there is no reason to choose electrodeposited WO_3 for direct intensity modulation unless switching speed is an extremely important parameter for the application at hand. The electrodeposited films are very rough and porous, which means that they need to be made much thicker to provide sufficient WO_3 on the surface for optimal contrast. If sufficiently thick films can be prepared at all, they have poor uniformity and adhesion to the support. Although we could reproduce the very high contrast recently reported for electrodeposited WO_3,[16] we managed to achieve this only in an aqueous electrolyte (proton intercalation), which leads to very unstable devices. In comparison, the sputtered WO_3 films can readily achieve a comparable contrast (at least ΔT = 93% in the red), without all the disadvantages associated with acid electrolytes.

Still, it should be kept in mind that electrodeposition is a very different method that does not require expensive equipment and can be performed directly on fabricated devices. For instance, different WO_3 films should be possible to pattern in a lithography-free manner on segmented or pixelated display devices. Furthermore, in electrochromic devices where the colors are not switched on or off, the electrodeposited WO_3 can be used to greatly improve the switching speed with only minor losses in other benchmark parameters. We have shown one such example by preparing a resonant nanocavity with electrodeposited WO_3 sandwiched between gold and platinum. The porous film morphology leads to an improvement in speed by more than one order of magnitude, while maintaining a brightness that is at least as high with a small loss of color quality. There are many recent examples of other structures in which the switching speed should be possible to improve in the same manner by changing to electrodeposited WO_3.[18,21−23] Overall, we believe this work will be helpful for the design of future devices utilizing inorganic electrochromism and the increased switching speed may enable more applications.

ASSOCIATED CONTENT

Supporting Information

The Supporting Information is available free of charge at https://pubs.acs.org/doi/10.1021/acsaom.2c00133.

Fresnel calculations, data for sol−gel films, photo of a colored sample, additional Raman spectra, XRD spectra, EIS data, switching data at different voltages, lifetime tests, and an additional chromaticity plot (PDF)

Video of switching (MP4)

AUTHOR INFORMATION

Corresponding Author

Andreas Dahlin − *Department of Chemistry and Chemical Engineering, Chalmers University of Technology, 41296 Gothenburg, Sweden;* orcid.org/0000-0003-1545-5860; Email: adahlin@chalmers.se

Authors

Marika Gugole − *Department of Chemistry and Chemical Engineering, Chalmers University of Technology, 41296 Gothenburg, Sweden*

Oliver Olsson − *Department of Chemistry and Chemical Engineering, Chalmers University of Technology, 41296 Gothenburg, Sweden*

Vandna K. Gupta − *Department of Chemistry and Chemical Engineering, Chalmers University of Technology, 41296 Gothenburg, Sweden*

Romain Bordes − *Department of Chemistry and Chemical Engineering, Chalmers University of Technology, 41296 Gothenburg, Sweden;* orcid.org/0000-0002-0785-2017

Elisabet Ahlberg − *Department of Chemistry & Molecular Biology, Gothenburg University, 41296 Gothenburg, Sweden;* orcid.org/0000-0002-4946-4979

Anna Martinelli − *Department of Chemistry and Chemical Engineering, Chalmers University of Technology, 41296 Gothenburg, Sweden;* orcid.org/0000-0001-9885-5901

Complete contact information is available at: https://pubs.acs.org/10.1021/acsaom.2c00133

Notes

The authors declare no competing financial interest.

■ ACKNOWLEDGMENTS

This work was financed by the Swedish Foundation for Strategic Research (Framework Grant EM16-0002). The authors thank the MyFab facilities and Michal Strach at the Chalmers Material Analysis Laboratory for support.

■ REFERENCES

(1) Xiong, K.; Tordera, D.; Jonsson, M. P.; Dahlin, A. B. Active control of plasmonic colors: emerging display technologies. *Rep. Prog. Phys.* **2019**, *82*, 024501.

(2) Jeon, N.; Noh, J.; Jung, C.; Rho, J. Electrically tunable metasurfaces: From direct to indirect mechanisms. *New J. Phys.* **2022**, *24*, 075001.

(3) Gu, C.; Jia, A.-B.; Zhang, Y.-M.; Zhang, S. X.-A. Emerging electrochromic materials and devices for future displays. *Chem. Rev.* **2022**, *122*, 14679−14721.

(4) Zhang, W.; Li, H.; Hopmann, E.; Elezzabi, A. Y. Nanostructured inorganic electrochromic materials for light applications. *Nanophotonics* **2020**, *10*, 825.

(5) Rai, V.; Singh, R. S.; Blackwood, D. J.; Zhili, D. A review on recent advances in electrochromic devices: a material approach. *Adv. Eng. Mater.* **2020**, *22*, 2000082.

(6) Kang, E. S. H.; Shiran Chaharsoughi, M.; Rossi, S.; Jonsson, M. P. Hybrid plasmonic metasurfaces. *J. Appl. Phys.* **2019**, *126*, 140901.

(7) Kim, Y.; Moon, C. W.; Kim, I. S.; Hyun, J. Active modulation of reflective structural colors. *Chem. Commun.* **2022**, *58*, 12014−12034.

(8) Neubrech, F.; Duan, X.; Liu, N. Dynamic plasmonic color generation enabled by functional materials. *Sci. Adv.* **2020**, *6*, No. eabc2709.

(9) Dyer, A. L.; Thompson, E. J.; Reynolds, J. R. Completing the color palette with spray-processable polymer electrochromics. *ACS Appl. Mater. Interface* **2011**, *3*, 1787−1795.

(10) Li, X.; Li, Z.; He, W.; Chen, H.; Tang, X.; Chen, Y.; Chen, Y. Enhanced electrochromic properties of nanostructured WO3 film by combination of chemical and physical methods. *Coatings* **2021**, *11*, 959.

(11) Bohnke, O.; Bohnke, C. l. Comparative study of the electrochromic properties of WO3 thin films. *Displays* **1988**, *9*, 199−206.

(12) Rezrazi, M.; Bohnke, O.; Pagetti, J. Electrochromic behavior of thin-films of tungsten trioxide prepared by anodic-oxidation of tungsten with pulsed current. *Displays* **1987**, *8*, 119−126.

(13) Leftheriotis, G.; Yianoulis, P. Development of electrodeposited WO3 films with modified surface morphology and improved electrochromic properties. *Solid State Ionics* **2008**, *179*, 2192−2197.

(14) Granqvist, C. G. Electrochromics for smart windows: Oxide-based thin films and devices. *Thin Solid Films* **2014**, *564*, 1−38.

(15) Gugole, M.; Olsson, O.; Xiong, K.; Blake, J. C.; Montero Amenedo, J.; Bayrak Pehlivan, I.; Niklasson, G. A.; Dahlin, A. High-contrast switching of plasmonic structural colors: inorganic vs organic electrochromism. *ACS Photonics* **2020**, *7*, 1762−1772.

(16) Cai, G.; Cui, M.; Kumar, V.; Darmawan, P.; Wang, J.; Wang, X.; Lee-Sie Eh, A.; Qian, K.; Lee, P. S. Ultra-large optical modulation of electrochromic porous WO3 film and the local monitoring of redox activity. *Chem. Sci.* **2016**, *7*, 1373−1382.

(17) Gugole, M.; Olsson, O.; Rossi, S.; Jonsson, M. P.; Dahlin, A. Electrochromic inorganic nanostructures with high chromaticity and superior brightness. *Nano Lett.* **2021**, *21*, 4343−4350.

(18) Wang, Z.; Wang, X.; Cong, S.; Chen, J.; Sun, H.; Chen, Z.; Song, G.; Geng, F.; Chen, Q.; Zhao, Z. Towards full-colour tunability of inorganic electrochromic devices using ultracompact fabry-perot nanocavities. *Nat. Commun.* **2020**, *11*, 302.

(19) Kim, K.-W.; Yun, T. Y.; You, S.-H.; Tang, X.; Lee, J.; Seo, Y.; Kim, Y.-T.; Kim, S. H.; Moon, H. C.; Kim, J. K. Extremely fast electrochromic supercapacitors based on mesoporous WO3 prepared by an evaporation-induced self-assembly. *NPG Asia Mater.* **2020**, *12*, 84.

(20) Hopmann, E.; Elezzabi, A. Y. Plasmochromic nanocavity dynamic light color switching. *Nano Lett.* **2020**, *20*, 1876−1882.

(21) Hopmann, E.; Carnio, B. N.; Firby, C. J.; Shahriar, B. Y.; Elezzabi, A. Y. Nanoscale all-solid-state plasmochromic waveguide nonresonant modulator. *Nano Lett.* **2021**, *21*, 1955−1961.

(22) Lee, Y.; Yun, J.; Seo, M.; Kim, S.-J.; Oh, J.; Kang, C. M.; Sun, H.-J.; Chung, T. D.; Lee, B. Full-color-tunable nanophotonic device using electrochromic tungsten trioxide thin tilm. *Nano Lett.* **2020**, *20*, 6084−6090.

(23) Li, Y.; van de Groep, J.; Talin, A. A.; Brongersma, M. L. Dynamic tuning of gap plasmon resonances using a solid-state electrochromic device. *Nano Lett.* **2019**, *19*, 7988−7995.

(24) Inamdar, A. I.; Kim, Y. S.; Jang, B. U.; Im, H.; Jung, W.; Kim, D.-Y.; Kim, H. Effects of oxygen stoichiometry on electrochromic properties in amorphous tungsten oxide films. *Thin Solid Films* **2012**, *520*, 5367−5371.

(25) Triana, C. A.; Granqvist, C. G.; Niklasson, G. A. Electrochromism and small-polaron hopping in oxygen deficient and lithium intercalated amorphous tungsten oxide films. *J. Appl. Phys.* **2015**, *118*, 024901.

(26) Saenger, M. F.; Hoing, T.; Robertson, B. W.; Billa, R. B.; Hofmann, T.; Schubert, E.; Schubert, M. Polaron and phonon properties in proton intercalated amorphous tungsten oxide thin films. *Phys. Rev. B* **2008**, *78*, 245205.

(27) Berggren, L.; Azens, A.; Niklasson, G. A. Polaron absorption in amorphous tungsten oxide films. *J. Appl. Phys.* **2001**, *90*, 1860−1863.

(28) Randin, J. P. Chemical and electrochemical stability of WO3 electrochromic films in liquid electrolytes. *J. Elec. Mater.* **1978**, *7*, 47−63.

(29) Yamada, Y.; Tabata, K.; Yashima, T. The character of WO3 film prepared with RF sputtering. *Sol. Energy Mater. Sol. C* **2007**, *91*, 29−37.

(30) Afify, H. H.; Hassan, S. A.; Obaida, M.; Moussa, I.; Abouelsayed, A. Preparation, characterization, and optical spectroscopic studies of nanocrystalline tungsten oxide WO3. *Opt. Laser Technol.* **2019**, *111*, 604−611.

(31) Antonaia, A.; Santoro, M. C.; Fameli, G.; Polichetti, T. Transport mechanism and IR structural characterisation of evaporated amorphous WO3 films. *Thin Solid Films* **2003**, *426*, 281−287.

(32) Rougier, A.; Portemer, F.; Quede, A.; El Marssi, M. Characterization of pulsed laser deposited WO3 thin films for electrochromic devices. *Appl. Surf. Sci.* **1999**, *153*, 1−9.

(33) Santato, C.; Odziemkowski, M.; Ulmann, M.; Augustynski, J. Crystallographically oriented mesoporous WO3 films: synthesis, characterization, and applications. *J. Am. Chem. Soc.* **2001**, *123*, 10639−10649.

(34) Lee, S.-H.; Cheong, H. M.; Tracy, C. E.; Mascarenhas, A.; Czanderna, A. W.; Deb, S. K. Electrochromic coloration efficiency of a-WO3-y thin films as a function of oxygen deficiency. *Appl. Phys. Lett.* **1999**, *75*, 1541−1543.

(35) Yu, H.; Guo, J.; Wang, C.; Zhang, J.; Liu, J.; Dong, G.; Zhong, X.; Diao, X. Essential role of oxygen vacancy in electrochromic performance and stability for WO3-y films induced by atmosphere annealing. *Electrochim. Acta* **2020**, *332*, 135504.

(36) Ho, C.; Raistrick, I. D.; Huggins, R. A. Application of A-C techniques to the Study of Lithium Diffusion in Tungsten Trioxide Thin Films. *J. Electrochem. Soc.* **1980**, *127*, 343−350.
(37) Wen, R.-T.; Granqvist, C. G.; Niklasson, G. A. Eliminating degradation and uncovering ion-trapping dynamics in electrochromic WO3 thin films. *Nat. Mater.* **2015**, *14*, 996−1002.
(38) Shen, P.; Tseung, A. C. C. Determination of the potential limits for WO3 colouration. *J. Mater. Chem.* **1994**, *4*, 1289−1291.

https://doi.org/10.1021/acsaom.2c00133
ACS Appl. Opt. Mater. 2023, 1, 558−568